

Chapter 6 - Geometrical Phase Shift in a Mesoscopic Ring due to Spin Orbit Interaction

Abstract

Spin-Orbit interaction induces a geometrical phase shift, which depends on the electron's trajectory. To study this effect we measure Aharonov-Bohm oscillation in the conductance of a mesoscopic GaAs/AlGaAs ring with a tilted magnetic field. For almost in-plane magnetic field we observe indications for a sharp jump of ϕ in the geometrical phase. The details, however, of the in-plane magneto-conductance are strongly sample-dependent.

The spin of a moving electron in solids is influenced by the lattice potential even when no external magnetic field is applied. This, so called, *spin - orbit* (SO) interaction originates from existing electric fields in the lattice reference frame being Lorentz transformed to a magnetic field in the reference frame of the moving electron. In this chapter we study the effect of SO interaction on the resistance of a mesoscopic ring with a tilted magnetic field. We discuss a possible interpretation of our results in terms of the *geometrical phase* that an electron acquires due to this interaction. Before describing the experiment we briefly review the theory of geometrical phase induced by SO interaction.

In an interference experiment one is usually interested in the phase change during a cyclic evolution of a wave function. Following the general treatment of Aharonov and Anandan [1], consider the cyclic evolution of the state $|\mathbf{y}(t)\rangle$ during the time interval $0 \leq t \leq \mathbf{t}$, which evolves according to the Schrödinger equation:

$$H(t)|\mathbf{y}(t)\rangle = i\hbar \frac{d}{dt} |\mathbf{y}(t)\rangle, \quad (6.1)$$

with $|\mathbf{y}(\mathbf{t})\rangle = \exp(i\mathbf{f})|\mathbf{y}(0)\rangle$, and \mathbf{f} is a real number. The total phase change, \mathbf{f} , can be written as a sum $\mathbf{f} = \mathbf{b}_d + \mathbf{b}_g$, where \mathbf{b}_d is the dynamical phase (or orbital phase):

$$\mathbf{b}_d = -\frac{1}{\hbar} \int_0^t dt \langle \mathbf{y}(t) | H | \mathbf{y}(t) \rangle , \quad (6.2)$$

and \mathbf{b}_g is the geometrical [2] phase:

$$\mathbf{b}_g = i \int_0^t dt \langle \tilde{\mathbf{y}}(t) | \frac{d}{dt} | \tilde{\mathbf{y}}(t) \rangle , \quad (6.3)$$

where $|\tilde{\mathbf{y}}(t)\rangle$ is defined as $|\tilde{\mathbf{y}}(t)\rangle = \exp[-if(t)]|\mathbf{y}(t)\rangle$, with $f(t)$ being an arbitrary real function satisfying $f(t) - f(0) = \mathbf{f}$. Note that this phase, \mathbf{b}_g , which is the non adiabatic generalization of the Berry phase [3], is not directly dependent on H and is independent of \hbar , namely this phase is finite in the classical limit.

In particular consider a cyclic evolution of a spin 1/2 particle with $\hat{u}(t) = \langle \mathbf{y}(t) | \boldsymbol{\sigma} | \mathbf{y}(t) \rangle$ being the unit vector indicating the direction of the spin, and $\boldsymbol{\sigma}$ is the Pauli spin matrix vector. Berry [3] found that the geometrical phase (6.3) in this case is given by:

$$\mathbf{b}_g = \frac{1}{2} \Omega , \quad (6.4)$$

where Ω is the solid angle that the closed curve on the unit sphere $\hat{u}(t)$ subtends at the origin.

Observable effects due to spin geometrical phase require non-uniform magnetic field. An intrinsic source of such field is provided by SO interaction. Taking into account SO interaction, the single electron Schrödinger equation is given by:

$$\left[\frac{\mathbf{p}^2}{2m} + V + \frac{\hbar}{4m^2c^2} (\nabla V \times \mathbf{p}) \cdot \boldsymbol{\sigma} \right] \mathbf{y} = E \mathbf{y} , \quad (6.5)$$

where $\mathbf{p} = (\hbar/i)\nabla - (e/c)\mathbf{A}$, \mathbf{A} is the electromagnetic vector potential, m is the free electron mass, V is the lattice periodic potential, $\boldsymbol{\sigma}$ is the Pauli spin matrix vector and the

other symbols have their usual meaning. The effect of SO interaction and external fields in semiconductors is best treated by the effective mass approximation [4]. In this approach the total wave function of an electron in the conduction band is described by: $\mathbf{y}(\mathbf{r}) = F(\mathbf{r})\mathbf{y}_c(\mathbf{r})$, where $\mathbf{y}_c(\mathbf{r})$ is the Bloch function at the bottom of the conduction band and $F(\mathbf{r})$ is the *envelope wave function* (EWF). Under the assumptions of this theory the Schrödinger equation for the EWF is given by:

$$[\mathbf{e}_c(\mathbf{p}) + U(\mathbf{r})]F_c(\mathbf{r}) = EF_c(\mathbf{r}) , \quad (6.6)$$

where $U(\mathbf{r})$ is the external potential (for the approximation to be valid this potential has to be smooth on the scale of the lattice constant). Thus, the effect of the periodic potential V , which appears explicitly in equation (6.5), is simulated by replacing the kinetic energy term $\mathbf{p}^2/2m$ with the function $\mathbf{e}_c(\mathbf{p})$. The number of independent constants in the expression of $\mathbf{e}_c(\mathbf{p})$ can be significantly reduced by considering the symmetry properties of the material in question, since $\mathbf{e}_c(\mathbf{p})$ must be invariant under the crystal symmetry point group.

In particular, the expansion of $\mathbf{e}_c(\mathbf{p})$ as a power series of \mathbf{p} for semiconductors having the zinc blende structure [5] was obtained by Ogg [6]. In these materials, which have no inversion symmetry, the conduction band splits into two spin subbands, and $\mathbf{e}_c(\mathbf{p})$ (which becomes a 2×2 matrix) contains terms which couple the spin and the spatial degrees of freedom of the electron. To lowest order in \mathbf{p} this interaction is given by:

$$H_b = \gamma \mathbf{s} \cdot \mathbf{k}(\mathbf{p}) , \quad (6.7)$$

where γ is a property of the material, $\mathbf{k}_x(\mathbf{p}) = \frac{1}{2\hbar^3} [p_x(p_y^2 - p_z^2) + (p_y^2 - p_z^2)p_x]$, and the other two components can be obtained by cyclic permutation. From equation (6.7) we see that the effect of SO interaction on an electron with a wave vector \mathbf{k} can be described

by an effective magnetic field given by: $\mathbf{B}_b = (\mathbf{g}/g^* m_B) \mathbf{k}(\mathbf{k})$, where g^* is the effective Lande g-factor and m_B is the Bohr magneton. Note that this magnetic field is perpendicular to the electron velocity (namely, $\mathbf{k}(\mathbf{p}) \cdot \mathbf{p} = 0$); its maximum value is obtained along the (110) direction (namely, $p_x = p_y$ and $p_z = 0$), and it vanishes along the high symmetry directions: (100) and (111).

The application of the effective mass theory derived for bulk semiconductors for estimating the effective magnetic field in two dimensional electron gas (2DEG) confined at the interface of a heterostructure is not well understood. One approach is to replace the operators p_z and p_z^2 , with \hat{z} being the unit vector normal to the interface (see Eq. (6.7)), by their expectation values with respect to the envelope wave function of the confined electron gas; namely, $p_z = 0$ and $p_z^2 = (\mathbf{p}\hbar / \Delta z)^2$, where Δz is the width of the wave function in the confinement direction [7]. However, if the interface is, for example, normal to the (001) direction, these substitutions correspond to an effective magnetic field **parallel** to the electron velocity; in contradiction with the relativistic picture of Lorentz transformation. Further complications arise when considering the effective magnetic field in a mesoscopic ring with narrow quasi one-dimensional channels. Nevertheless, we can use the well-known values of \mathbf{g} and g^* for bulk semiconductors to estimate at least the order of magnitude of the effective magnetic field in the confined 2DEG. These constants can be calculated by the Kane model [8], extended to include the coupling of the conduction s - like band Γ_{6c} with the upper valence bands, $\Gamma_{7v} - \Gamma_{8v}$ (heavy and light hole bands), and the p - like conduction bands, $\Gamma_{7c} - \Gamma_{8c}$, both lying above the Γ_{6c} band [9]. For 2DEG confined in a GaAs - AlGaAs heterostructure with electron density of $2 \times 10^{11} \text{ cm}^{-2}$ we find that along the (110) direction $B_b = 0.9 \text{ T}$.

Similarly to the above described case, where the electric field is that of the lattice, the confining electric field at the interface of a heterostructure, E_z , leads to an additional term in the effective Hamiltonian [10]:

$$H_i = (\alpha E_z / \hbar)(\mathbf{s} \times \mathbf{p}) \cdot \hat{\mathbf{z}}, \quad (6.8)$$

where α is a property of the material. Note that the effective magnetic field associated with this interaction, B_i , is isotropic in the plane of the 2DEG. For a 2DEG confined in a GaAs - AlGaAs heterostructure with electron density of $2 \times 10^{11} \text{ cm}^{-2}$ we find $B_i = 0.4 \text{ T}$ normal to the electron momentum. Thus, the spin orbit in this system is dominated by the bulk term. This conclusion is consistent with measurements of weak antilocalization-like magnetoresistance [11].

Consider the effect of SO interaction on the spin of an electron moving around a mesoscopic ring [12]. According to the adiabatic approximation the orientation of the spin follows the direction of the momentum dependent effective magnetic field. This approximation is valid when the spin precession time is much shorter than the traveling time of the electron around the ring, i.e. $c \equiv \hbar v / g^* m_B B a \ll 1$ [13], where v is the electron velocity, B is the effective magnetic field, a is the radius of the ring, and the transport along the ring is assumed to be ballistic. The general non adiabatic case can be treated by a numerical approach or even analytically in special cases of high symmetry [14], however, for simplicity, we consider here only the adiabatic case. The geometrical phase for this case is half the solid angle subtends by the closed curve $\mathbf{B}(t)$ (see Eq. (6.4)), which describes the magnetic field in the electron reference frame along the motion around the ring.

A special case of interest is when $\mathbf{B}(t)$ lies in the plane of the 2DEG. In this case the geometrical phase is given by $\mathbf{b}_g = \mathbf{g}[\mathbf{B}(t)]\mathbf{p}$, where $\mathbf{g}[\mathbf{B}(t)]$ is the winding number of the curve $\mathbf{B}(t)$ around the origin [3]. Thus, in the absence of an external magnetic field,

$\mathbf{b}_g = \mathbf{p}$. Consider now the geometrical phase in the presence of an external magnetic field, B_{ext} , applied *in the plane* of the ring. For $B_{ext} < B_{SO}$, where B_{SO} is the effective SO magnetic field in the direction of B_{ext} , we expect $\mathbf{b}_g = \mathbf{p}$, while as B_{ext} increases and approaches B_{SO} a sharp transition to a regime with $\mathbf{b}_g = 0$ is expected to occur (see Fig. 6.1) [3, 15]. Note that this simple theoretical picture completely ignores orbital effects due to in-plane field. This is justified only if the magnetic length l is much larger than the width of the 2DEG wave function in the confinement direction Δz . In our experiment $l/\Delta z = 1.8$ at $B = 2$ T, thus this simplification assumption is not fully justified.

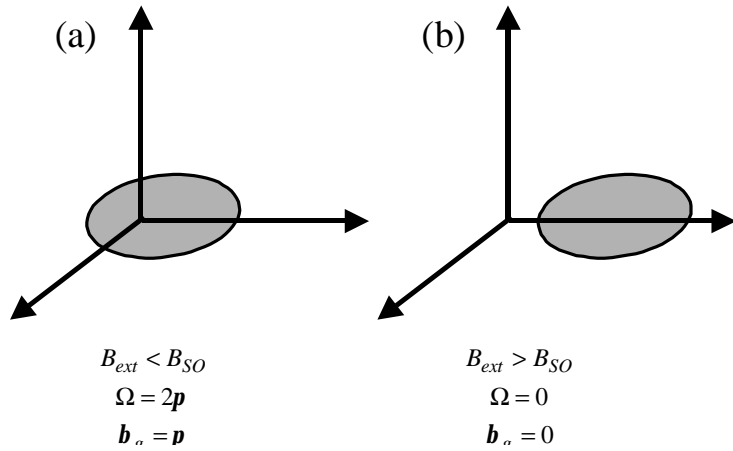


Fig. 6.1 The curve $\mathbf{B}(t)$ for (a) $B_{ext} < B_{SO}$ and for (b) $B_{ext} > B_{SO}$

Our device, seen schematically in the inset of Fig. 6.2, contains an AB ring with diameter 1.1 mm patterned on the surface of a GaAs-AlGaAs heterostructure supporting 2DEG with density $n_s = 3.2 \cdot 10^{11} \text{ cm}^{-2}$ and mobility $\mathbf{m} = 1.2 \cdot 10^6 \text{ cm}^2/\text{Vs}$ (at $T = 4.2 \text{ K}$) formed 70 nm below the surface. Longitudinal resistance and Hall resistance are measured using a 4-probe configuration (see inset of Fig. 6.2) with an injected current of $I = 1 \text{ nA}$ at a temperature $T \approx 100 \text{ mK}$. Fig. 6.2 shows AB oscillation in the resistance of

the device as a function of normally applied magnetic field with the expected period $\Delta B = \Phi_0/A = 4.3 \text{ mT}$, where A is the area of the ring. The Hall resistance indicates the filling factor ν in the bulk of the 2DEG.

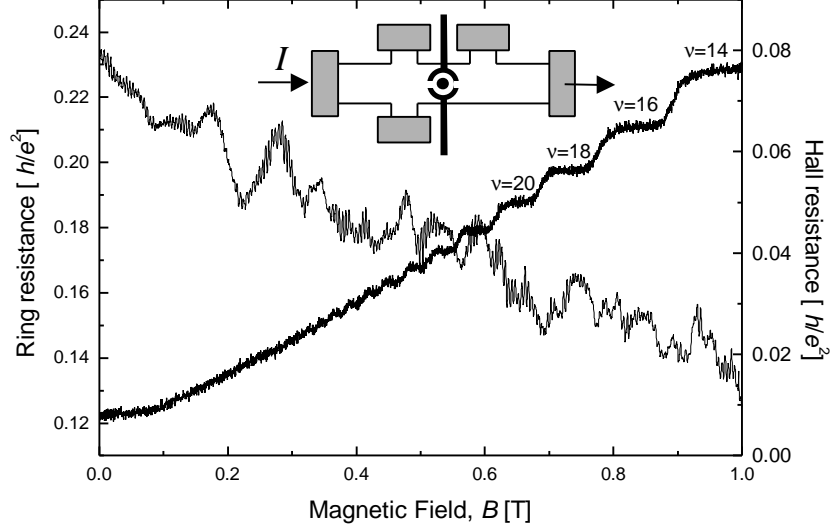


Fig. 6.2 The longitudinal resistance shows AB oscillation as a function of a normally applied magnetic field. The Hall resistance indicates the filling factor in the bulk of the 2DEG.

Observation of effects due to SO geometrical phase with a normal magnetic field is very difficult. While the AB phase changes by π with an applied normal field of $\Phi_0/2A$, the same change in the geometrical phase requires changing the field from zero to infinity (see Eq. (6.4)). On the other hand, tilting the direction of the magnetic field from the normal to the sample direction weakens the dependence of AB phase on the applied field, thus facilitating the observation of effects due to the geometrical phase. Figure 3 shows the measured periodicity ΔB of AB oscillation (expressed in terms of effective area, namely $A_{eff} = \Phi_0/\Delta B$) as a function of magnetic field applied with an angle θ with respect to the plane of the ring (see Fig. 6.3 inset). For these values of θ we find regular

AB oscillation with a period proportional to $\sin \mathbf{q}$, indicating, thus, no effect due to the in-plane component of the magnetic field.

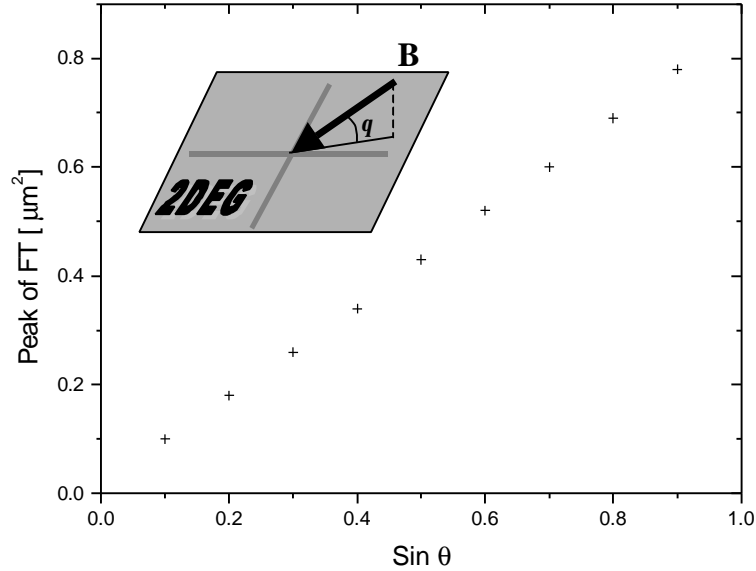


Fig. 6.3 Periodicity of AB oscillation with a tilted magnetic field. The angle between the magnetic field and the plane of the 2DEG is \mathbf{q} .

Deviations from a regular AB oscillation are observed only with smaller values of \mathbf{q} , namely, almost in-plane magnetic field. Fig. 6.4 shows magneto resistance data taken with 4 different values of \mathbf{q} . In all traces we find irregular behavior near $B_c \approx 2.3 \text{ T}$. The amplitude of AB oscillation near B_c is reduced and the resistance oscillates faster as a function of B near this point. Note that the period of oscillation on both sides of B_c is as expected from the AB effect, namely $\Delta B = \Phi_0 / A \sin \mathbf{q}$. To a good approximation the oscillation above B_c are out of phase with respect to the oscillation below B_c , indicating an extra phase \mathbf{p} acquired by passing the point B_c .

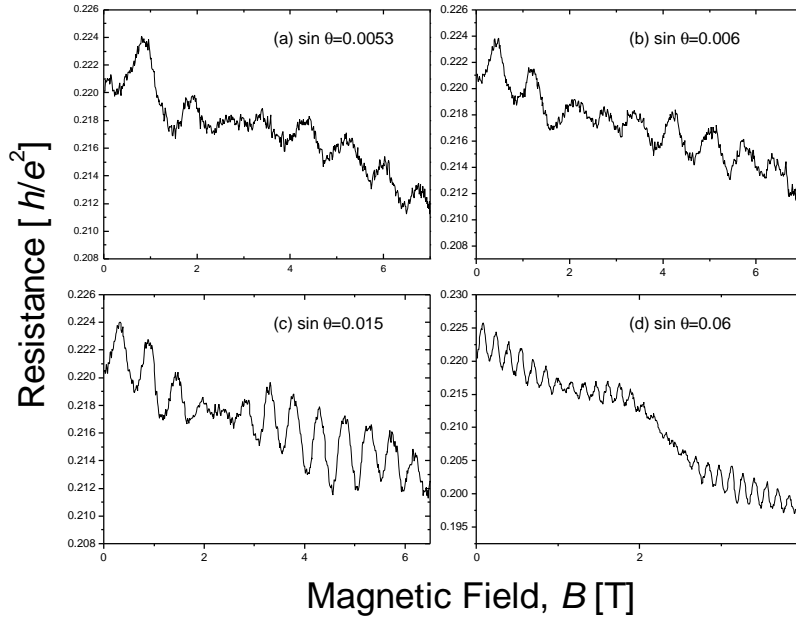


Fig. 6.4 Magneto resistance of the ring for 4 small values of q . Note the irregular behavior near $B_c = 2.3$ T.

The observations seen in Fig. 6.4 are in good agreement with the simple theoretical picture presented in Fig. 6.1, thus suggesting that B_c has to be identified with B_{SO} . As far as we know, there is no other physical mechanism that can account for these observations. Note, however, that the behavior seen in Fig. 6.4 is sample dependent. As in the present device, we found deviations from a regular AB oscillation at small q in the other two devices that we measured, however, the detailed behavior was different. To understand this it is important to understand the range of validity of the simple theoretical picture presented above and the conditions for experimental observation.

The actual rings in the experiment support a few 1D channels. Note that B_{SO} depends on the electron velocity v which is different for different channels. A strong mixing

between channels will strongly modify the effect of SO interaction on the measured magneto resistance. For weak mixing, on the other hand, one expects to observe a set of irregular points associated with the different values of B_{SO} for different channels. The fact that only one irregular point is observed in Fig. 6.4 suggests that magneto resistance oscillation in this device is dominated by a single channel.

In order to compare between different channels we consider adiabaticity, thermal smearing and SO scattering. On one hand the adiabaticity condition $c \ll 1$ is better fulfilled for channels with smaller velocity. On the other hand, the onset temperature for thermal smearing, $k_B T_s \approx h v / L$ (L is a typical length difference between interference paths), is proportional to v , thus, thermal smearing is stronger for channels with smaller velocity. In GaAs the main spin relaxation mechanism is due to spin precession about the effective SO magnetic field [11]. The direction and magnitude of this field, which depend on the electron momentum, vary as the electron is elastically scattered by impurities. We estimate the corresponding spin relaxation time in our device to be $t_s \approx 15$ ps [11]. Since this time has to be compared with the traveling time around the ring, we find that the effect of scattering is stronger for channels with smaller velocity. Combining these considerations may lead to a single dominant channel.

In conclusion, we study SO effects on magnetoresistance of a mesoscopic ring with a tilted magnetic field. For small angles between the external field and the plane of the ring we find irregular AB oscillation. The observed irregularity in one device can be explained in terms of a sharp change of \mathbf{p} in the geometrical phase. To explain why such a behavior was not observed in other devices we show that strong mixing between channels may inhibit observation of this effect.

References

- [1] Y. Aharonov and J. Anandan, Phase Change During a Cyclic Quantum Evolution, *Phys. Rev. Lett.* **58**, 1593 (1987).
- [2] The interpretation of this phase in terms of a geometrical parallel transport was given by: B. Simon, Holonomy, the Quantum Adiabatic Theorem, and Berry's Phase, *Phys. Rev. Lett.* **51**, 2167 (1983).
- [3] M. Berry, Quantal Phase Factors Accompanying Adiabatic Changes, *Proc. Roy. Soc. London, Ser. A* **392**, 45 (1984).
- [4] J. Luttinger and W. Kohn, Motion of Electrons and Holes in Perturbed Periodic Fields, *Phys. Rev* **97**, 869 (1955).
- [5] G. Dresselhaus, Spin-Orbit Coupling Effects in Zinc Blende Structure, *Phys. Rev.* **100**, 580 (1955).
- [6] N. Ogg, Conduction-Band g Factor Anisotropy in Indium Antimonide, *Proc. Phys. Soc.* **89**, 431 (1966).
- [7] F. Malcher *et al.*, Electron States in GaAs/GaAlAs Heterostructures: Non-Parabolicity and Spin-Splitting, *Superlattices and Microstructures* **2**, 267 (1986).
- [8] E. Kane, Band Structure of Indium Antimonide, *J. Phys. Chem. Solids* **1**, 249 (1957).
- [9] P. Pfeffer and W. Zawadzki, Conduction Electrons in GaAs: Five-level $\mathbf{k} \cdot \mathbf{p}$ Theory and Polaron Effects, *Phys. Rev. B* **41**, 1561 (1990).
- [10] Yu. Bychkov and E. I. Rashba, Oscillatory Effects and the Magnetic Susceptibility of Carriers in Inversion Layers, *J. Phys. C* **17**, 6039 (1984).
- [11] P. Dresselhaus *et al.*, Observation of Spin Precession in GaAs Inversion Layers Using Anti-Localization, *Phys. Rev. Lett.* **68**, 106 (1992).
- [12] A. Aronov and Y. Lyanda - Geller, Spin-Orbit Berry Phase in Conducting Rings, *Phys. Rev. Lett.* **70**, 343 (1993).

- [13] A. Stern, Berry's Phase, Motive Forces, and Mesoscopic Conductivity, Phys. Rev. Lett. **68**, 1022 (1992).
- [14] Tie-Zheng Qian and Zhao-Bin Su, Spin-Orbit Interaction and Aharonov-Anandan Phase in Mesoscopic Rings, Phys Rev. Lett. **72**, 2311 (1994).
- [15] Y. Lyanda - Geller, Topological Transitions in Berry's Phase Interference Effects, Phys. Rev. Lett. **71**, 657 (1993).